THE UNIVERSITY of EDINBURGH

Edinburgh Research Explorer

The influence of wind and the spatial layout of dwellings on fire spread in informal settlements in Cape Town

Citation for published version:
Gibson, L, Cicione, A, Stevens, S & Rush, D 2022, 'The influence of wind and the spatial layout of dwellings on fire spread in informal settlements in Cape Town', *Computers, Environment and Urban Systems*, vol. 91, 101734. https://doi.org/10.1016/j.compenvurbsys.2021.101734

Digital Object Identifier (DOI):
10.1016/j.compenvurbsys.2021.101734

Link:
Link to publication record in Edinburgh Research Explorer

Document Version:
Peer reviewed version

Published In:
Computers, Environment and Urban Systems

General rights
Copyright for the publications made accessible via the Edinburgh Research Explorer is retained by the author(s) and / or other copyright owners and it is a condition of accessing these publications that users recognise and abide by the legal requirements associated with these rights.

Take down policy
The University of Edinburgh has made every reasonable effort to ensure that Edinburgh Research Explorer content complies with UK legislation. If you believe that the public display of this file breaches copyright please contact openaccess@ed.ac.uk providing details, and we will remove access to the work immediately and investigate your claim.

OPEN ACCESS

Download date: 09. Jun. 2023

The influence of wind and the spatial layout of dwellings on fire spread in informal settlements in Cape Town.

Abstract

Fires in informal settlements are devastating to residents of these precarious urban environments. This paper highlights the use of spatial metrics and wind speed and direction for fire spread risk identification for informal settlement fires in Cape Town. Data on: fire incidents, dwelling footprints, and the wind conditions during a fire, are analysed both together and separately. Fire incidence data analysed with wind data reveals that the majority of fires occur in December with the most destructive fires taking place during moderate wind conditions. At higher wind speeds, the distance between the flame and adjacent dwelling is not reduced but the flame height is, leading to reduced radiation. Also, convective cooling at higher wind speeds increases the time-to-ignition and flashover of the adjacent dwelling. Analysis of dwelling data reveals that the average and standard deviation of distance to the first nearest neighbour together with edge density can be used to identify areas at risk of fire spread. A threshold approach using the distance to a dwelling's first nearest neighbour together with the range in distance from the dwelling's first to third nearest neighbours allow for the identification of specific dwellings within a settlement which are at risk of fire spread.

Introduction

Fires in informal settlements can result in thousands of people being left homeless in a single event and are recognised as a disaster in the developing world [1]. Cape Town is informally known as the fire capital of South Africa [2], whilst at the same time, Cape Town is well known for its strong winds. In this paper, the combination of fire and wind is explored in informal settlements in Cape Town. Wind is thought to have significant, though varied, effect on informal settlement fires. In the early stages of a fire in a single dwelling, strong winds may delay or even prevent flashover from occurring by increasing the required compartment heat release rate needed for the onset of flashover [3]. However, once a fire is fully developed in a dwelling, wind can contribute to through draft conditions which may increase the extent and heat release rate of a flaming plume venting from the windows or doors [4]. This not only reduces the time of fire spread to the closest neighbouring dwellings, but also enables the fire to spread across larger gaps between dwellings. Furthermore, it is widely known that wind increases oxygen supply, which leads to more rapid burning and creates air pressure differences that push flames and fire brands in the direction of new fuels. This 'pushing' effect [5] results in an increased flame tilt angle (i.e. the angle between the centre line of the flame ejecting from the burning dwelling and the burning dwelling itself), which decreases the distance between the flames of the burning dwelling and the adjacent dwelling. Data on the weather conditions at the time of a fire incident together with the damage caused by the fire can be used to explore these assertions for informal settlement fires in Cape Town.

It has been stated by Walls et al. [6] that fire spread between dwellings occurs rapidly due to the close proximity of dwellings to each other as well as dwelling density, both of which vary from settlement to settlement. Therefore, the risk of fire spread is likely to vary from settlement to settlement dependant on these factors. Within-settlement variations in dwelling proximity and density will also contribute to varying within-settlement risk. Dwelling proximity can be represented by the distance of a dwelling to its nearest neighbour. Although the position of openings in the dwellings may exacerbate fire spread, all else being equal, it can be assumed that fire will spread to the object in closest proximity to the radiation source or flame.

Spatial metrics can be used to describe morphological characteristics within the urban environment [7] and can be used to challenge or confirm assertions such as " Fires spread rapidly through such densely populated areas" [8], "Fires can start and spread easily in such locations due to a number of factors, including: ….high building density…" [9], and "…easily spread from one dwelling to another based on the close proximity of adjacent houses…." [8]. Thus from the perspective of fire spread, spatial metrics which consider dwelling density and proximity can be analysed against areas where historic fires have occurred. Thus in a further advancement of the understanding of fire spread risk, spatial metrics calculated for the historic fire areas are used to determine thresholds above or below which an area may be considered at risk of fire spread and at risk areas in informal settlements in Cape Town are identified on this basis.

This research uses data from four independent sources to explore relationships between number of fire incidences and size of fires, time of year, weather conditions, and dwelling layouts: (1) a third party fire incidence dataset consisting of all recorded fire incidents (~99 000 records) within the City of Cape Town from 2009 to 2015, (2) hourly weather data for 10 years recorded by South African Weather Services at Cape Town International Airport, (3) dense time series of Sentinel-2 satellite images (64 images) to map historic fires and Google Earth historic imagery to assist in validation, and (4) informal dwelling outlines captured digitally from high resolution aerial photography for all informal settlements in Cape Town (~115 000 polygons).

Method

The method (Figure 1) is divided into three subsections: (i) Fire incidence data collected by the City of Cape Town and weather data recorded by South African Weather Service is firstly analysed to understand the relationship between the size of fires, the month, and wind conditions. (ii) Remote sensing of dense time series Sentinel-2 data to map recent large historic informal settlement fires. (iii) Spatial metrics from the informal settlement dwellings for the fire areas mapped from remote sensing and threshold parameters for these metrics are obtained for the fire affected areas. These threshold parameters are applied to spatial metrics calculated for all informal settlement areas in Cape Town, and at risk areas are highlighted. Finally, the findings of each of the subsections are drawn together in the discussion. Here the effect of the wind speed on flame tilt angle and radiation is expanded and related to the risk parameters identified in the spatial metrics analysis. It must be noted that data on fire suppression with respect to the size of the fire prior to intervention is unknown. Thus, linkages to suppression activity cannot be made.

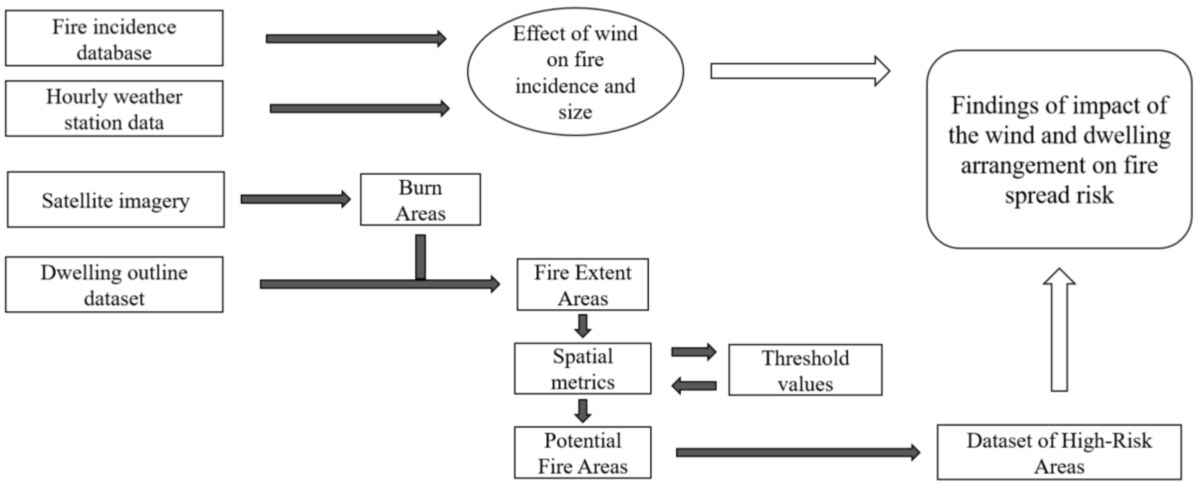

Figure 1. Flowchart of methodology.

An overview map highlighting the settlements and locations mentioned in this paper is shown in Figure 2 for reference.

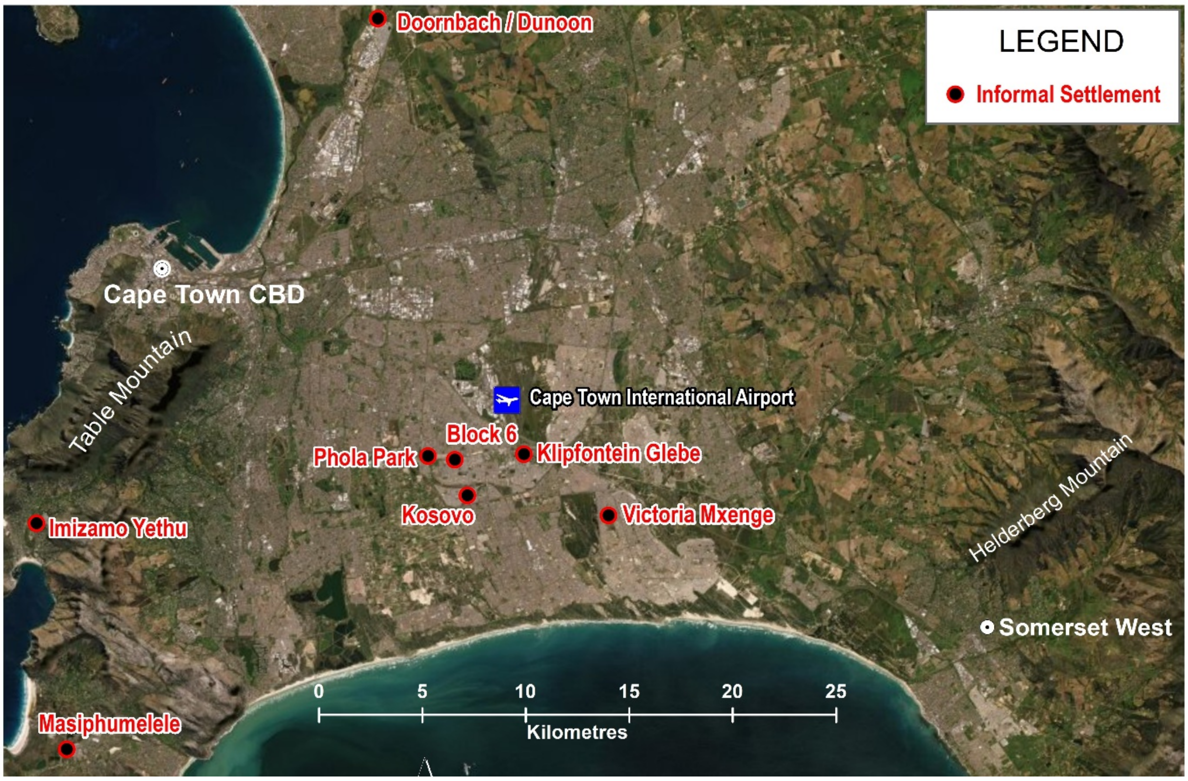

Figure 2. Overview map indicating settlements mentioned in the paper and the location of Cape Town International Airport

Fire incidence and the wind:

The City of Cape Town collects and makes available to the public, all fire incidents to which city officials respond [10]. Data is currently available from 01 January 2009 to 31 December 2017 but due to data being inconsistently captured, only data from 01 January 2009 to 31 December 2015 is analysed as this represented the longest period of consistent capture of complete calendar years. Further, a manual data sorting and cleaning process is necessary to correctly classify all informal settlement fires.

Hourly wind speed and direction data measured at a height of 10 m, obtained from South African Weather Services station at Cape Town International Airport are analysed against the fire incidence database. This weather station was selected since it, like most informal settlements in Cape Town, is located on the Cape Flats – a sandy plain stretching from the Table Mountain range in the west to the Helderberg Mountains in the East (mountain range in proximity of Somerset West on Figure 2). Wind conditions at Cape Town International Airport are thus likely to be representative of most informal settlements in Cape Town. The fire incidence data is matched to the weather station data using the time that the first call was received and wind data for the corresponding hour is analysed. The wind data can be analysed with the number of structures destroyed in each fire to test the extent wind speed and direction plays in the destruction wreaked by a fire.

Remote sensing:

Gibson et al [11] describe the change in reflectance of the Sentinel-2 Blue Band both at pixel level and cluster level across a time series to flag potential fires (Fire Extent Areas). Sentinel-2 was first launched in June 2015 and cloud free images of the study area were selected from that date onwards resulting in a dense time series of 64 images ranging in date from 16 February 2016 to 5 February 2019. The approach at pixel level relies on the sudden decrease in reflection in the immediate aftermath of a fire, as homes are burned and charred, followed by a sudden increase in reflection as old roofs are replaced with new metal roofs. At cluster level, the edge of the fire is detected through analysing the standard deviation in reflection between a pixel and its neighbours. A rapid change in the standard deviation implies a sudden change in reflection for either a pixel or its neighbours and together with the change in reflection at pixel level, is used to flag a potential fire. These flags (Fire Extent Areas) are validated using a combination of Google Earth historical imagery to confirm the fire incident and approximate date, media reports of fire, and City of Cape Town high resolution aerial photography [12]. Using these stringent criteria, only true fire events are recorded and all false positives, such as those which occur through settlement expansion and densification, are removed. It is also possible to identify large fires which occurred before the date of the first image capture due to the high reflectance values of new roofs which were then verified against the fire incidence database.

A spatial layer of informal dwelling footprints [13] for informal settlements in the City of Cape Town has been digitised through visual interpretation at a scale of 1: 200 from high resolution aerial photography captured by the City of Cape Town [12]. This layer is used to extract the dwellings affected by each of the identified historic fires. The actual aerial extent of the fires (Fire Extent Area) is obtained through drawing nearest neighbour connecting lines (using the proximity tools in ArcMap 10.5) between dwellings affected by the fire and using these lines together with the outlines of the dwellings themselves to create Fire Extent Area polygons for each fire, as depicted in Figure 3.

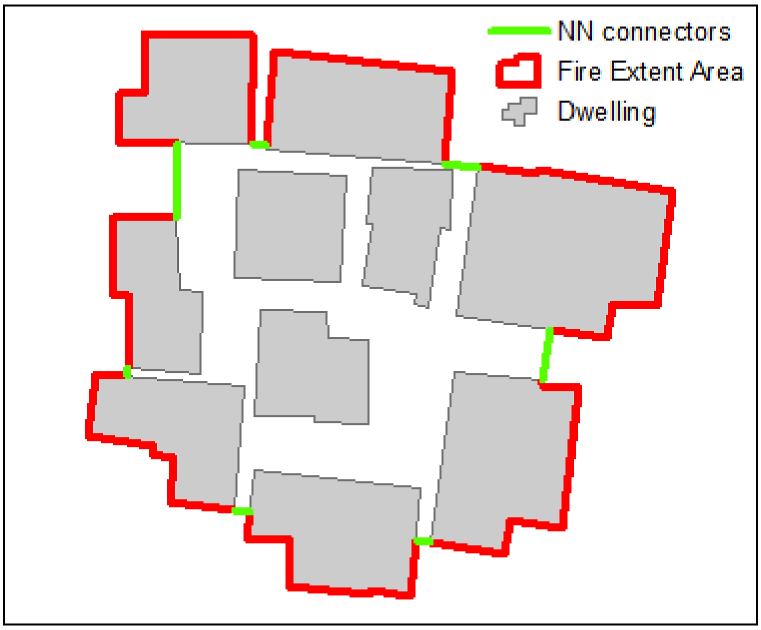

Figure 3. Fire Extent Area polygons are created with nearest neighbour (NN) connectors between dwellings affect by fire and, combined with the dwelling polygons, using these lines as the outermost boundary of the fire.

Spatial metrics:

Using the historic fire areas, spatial metrics for each Fire Extent Area are calculated to provide insight into the hypothesis that dwellings in close proximity and/or areas with high dwelling density promote the spread of informal settlement fires and can highlight both settlements at risk and within-settlement risk.

To apply insights discovered through the spatial metrics analysis of Fire Extent Areas to the informal settlements in Cape Town, a geographical unit of analysis (GUA) must be determined. The most obvious choice of GUA would be a settlement but since individual settlements can vary significantly in size and many variations of spatial arrangement can be present within settlements, local variations will be lost if such a broad approach is taken. For example, a settlement may have a high dwelling density in part of the settlement (potentially representing high risk) and low density in other parts (representing low risk) however if the calculations of density metrics are carried out at settlement scale, an average density will be returned in this scenario, missing identification of both high and low risk within the settlement.

Therefore, a way of subdividing settlements into a meaningful GUA within the context of informal settlement fire is needed. A fire spread pathway approach [14] to identify the maximum fire size (assuming no intervention) that could occur using critical separation distance is selected. Cicione et al (in 3 separate papers, using 3 different techniques, i.e. from experiments measurements [15], from FDS simulations [16] and from robust analytical equations [17]) and Wang et al [18] independently estimated a critical separation of approximately 3 m for informal settlements in Cape Town. Thus, a critical separation distance of 3 m was selected to determine the geographical unit of analysis.

The creation of the GUAs involve buffering all dwellings by half the critical separation distance (i.e. 1.5 m) which then determines which dwellings pose a risk to each other in event of a fire as the method connects all dwellings within the critical separation distance of each other. Buffering back by the same distance, creates polygons of dwellings at risk of fire spread from each other. This method is visually illustrated in Figure 4. The buffering back by -1.5m is important in spatial metric calculations as the border of the GUA should correspond with the outermost perimeter of the dwellings on the edge of the GUA and the inter-dwelling spaces where dwellings are within 3m of each other are included in the GUA.

Therefore, for delineating units of analysis, dwellings are buffered by 1.5m and the resulting dataset in turn buffered by -1.5m. The buffer lines are dissolved, and this results in polygons which can be considered the "Potential Fire Areas" and can be used as the GUA for the purposes of this research. If a smaller critical separation distance were to be used, then the number of potential fire areas would increase with an increase in the frequency of small Potential Fire Areas (PFAs). Should a larger separation distance be used, more large PFAs would be created with the total number of PFAs reduced.

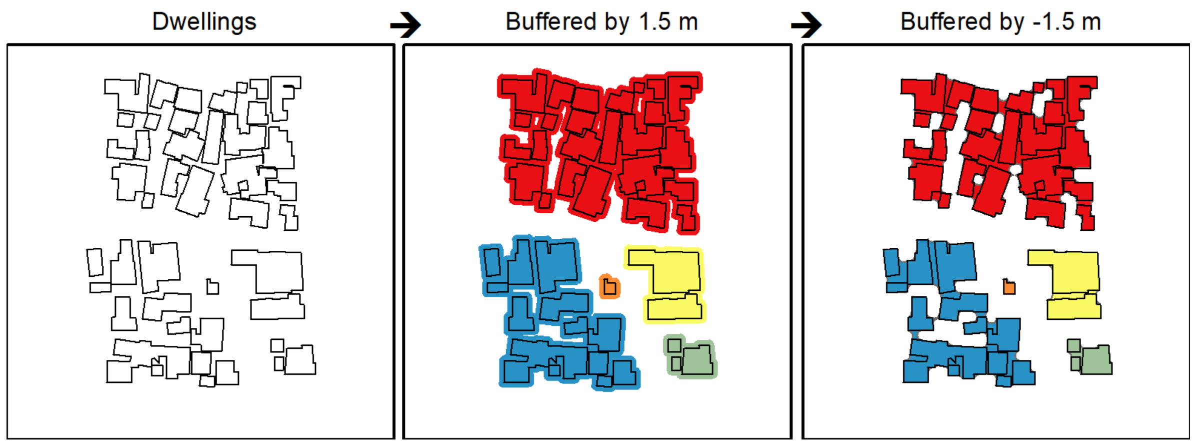

Figure 4. Method used to create Potential Fire Areas. Different colours represent different Potential Fire Areas.

Landscape density (PLAND), Euclidean nearest neighbour distance (ENN) and edge density (ED) metrics were first investigated for informal settlement fires by Gibson et al.[19] and diagrams illustrating the calculation of the metrics are shown in that publication should the reader require further information. Here, these spatial metrics are calculated for the historic Fire Extent Areas obtained from remote sensing, and statistical analyses of these metrics are carried out. Expanding on the nearest neighbour metrics, normalised density of distances to dwellings' first, second and third nearest neighbours (calculated using the proximity tool "Generate Near Table" in ArcGIS 10.5 and illustrated in Figure 5) can be considered in conjunction with the previously described spatial metrics.

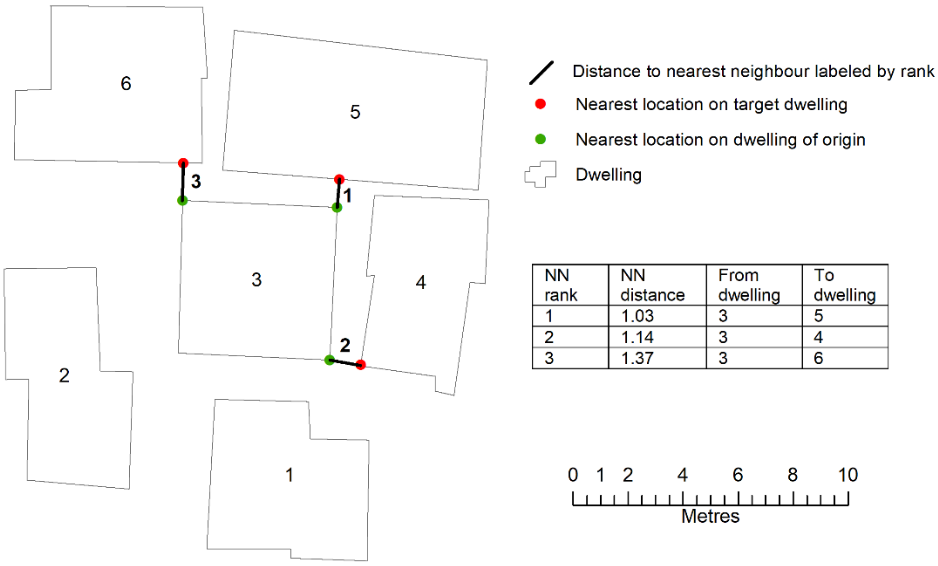

Figure 5. Illustration of a dwelling's first three nearest neighbours using dwelling 3 as an example. The points on the dwelling of origin located closest to its neighbours are marked as a point, as is the point on the target dwelling.

Normalised density of distance to dwellings' first, second and third nearest neighbours are calculated for the Fire Extent Area and compared against the normalised distances to neighbours in Potential Fire Areas and for all dwellings in the informal settlement dwelling database. Analysis of dwellings distance to first ENN against the range in distance from the same dwelling's third ENN to first ENN is carried out for the Fire Extent Areas. Note that if the nearest neighbour is less than 10 cm, then the dwellings are assumed to be touching (the resolution of the aerial photography prevents precision below this value) and therefore multiple dwellings may be depicted as a single polygon. Threshold parameters obtained using the 75th percentiles of the range of values found in all Fire Extent Area are then applied to the "Potential Fire Areas" dataset to identify those areas deemed at risk on the basis of the spatial metrics. The percentile approach, rather than a maximum and minimum approach is to remove outliers from the analysis and the 75th percentile is used as this includes of the majority (75%) of measurements.

Results

This section is also subdivided into three subsections, namely: (i) Fire incidence and wind data, (ii) Fire Extent Areas, and (iii) Spatial metrics, with each subsection discussing the results of the corresponding method discussed above.

Fire incidence and wind data

Monthly analysis of the fire incidence database (2009 – 2015) of the total number of fires (Figure 6.a) and the number of structures destroyed in an individual fire by month (Figure 6.b), show that the majority of fires occur in December (count 278) followed by November (count 189). June, August and September have the lowest total number of fire incidents recorded with counts of 96, 95 & 95 respectively. The number of structures destroyed presents a slightly different picture, however it must be noted that number of structures destroyed is estimated in the database and thus the accuracy of these numbers cannot be ascertained. However, as with the number of incidents, the highest number of structures destroyed is in December (count 2131, note anomalously high points in Figure 6.b) followed by November (count 2061). Anomalously, 1825 structures were destroyed in May, largely due to a single fire in Masiphumelele in May 2014, which can be seen as an outlier in Figure 6.b.

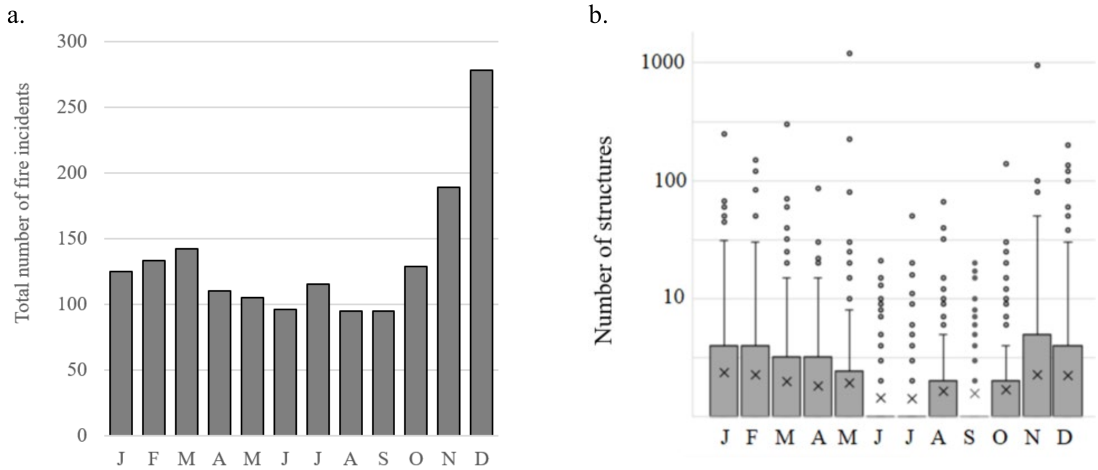

Figure 6. a. Number of fire incidences per month and b. Number of structures destroyed in individual fires by month (note the log scale) from the City of Cape Town Fire Incidence Database.

On the assumption that large fire spread is partially caused by high wind speed, the wind data from 1 January 2009 to 31 December 2019, displayed in the box-and-whisker chart (Figure 7) confirms that November and December are indeed amongst the windiest months. Box-and-whisker charts divide the data into quartiles, thus the median line (50% percentile) is the line in the middle of the box with the upper and lower boundaries of the box representing the 75th and 25th percentile respectively. The whiskers represent the variation in the data outside of the first and third quartiles with the upper whisker plotted at the 75th percentile plus 1.5 times the interquartile range (or the maximum, whichever is lower). Similarly, the lower whisker is drawn at the 25th percentile minus 1.5 time the interquartile range (or the minimum, whichever is higher). Outliers are shown as points above or below the whiskers. January is recorded as the windiest month on average, however the number of fires (count 125) and the number of structures destroyed (972) do not reflect this.

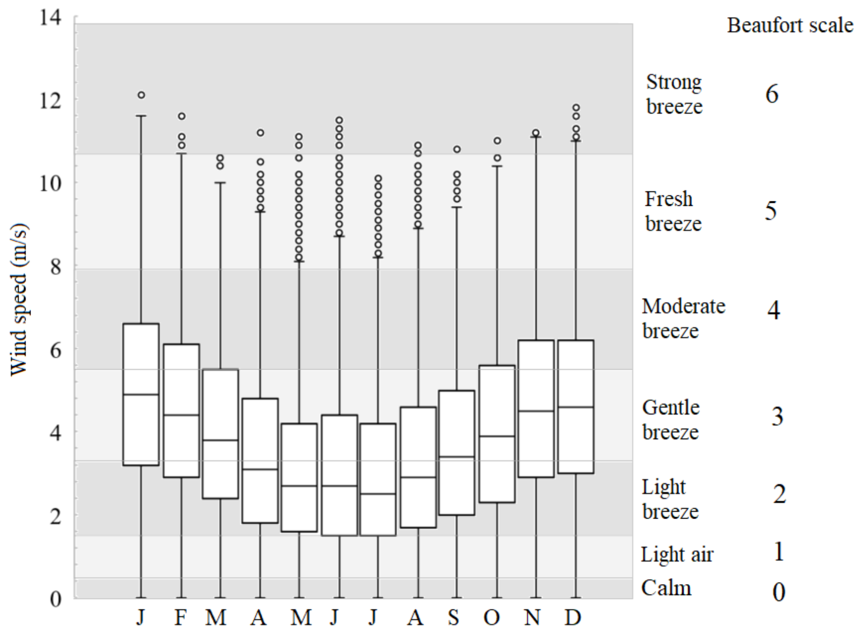

Figure 7. Box-and-whisker plot of wind speed by month at Cape Town International Airport (data from 1 Jan 2009 – 31 Dec 2019).

A box-and-whisker plot of the wind speed at the time of the fire incident against the number of structures destroyed (Figure 8.a and similarly represented on Figure 8.b) does not allow for the simplistic conclusion that the higher the wind speed, the more structures destroyed. Rather, it can be seen that the most destructive fires occur at Beaufort Scale 2 (Light Breeze, 1.6 – 3.3 $m.s^{-1}$) with fires destroying more than 100 structures not occurring in lighter wind conditions. The mean (marked with an x on Figure 8.a) and median number of structures destroyed are similar for Beaufort Scale 2, 3 (Gentle breeze, 3.4 – 5.5 $m.s^{-1}$) and 4 (Moderate Breeze, 5.6 – 7.9 $m.s^{-1}$), with some large destructive fires still occurring at the higher wind speeds corresponding to Beaufort Scale 5 (Fresh Breeze, 8.0 – 10.7 $m.s^{-1}$) albeit less frequently. Figure 8.b shows the most destructive fires (on average) occur at around 3 $m.s^{-1}$ (Beaufort Scale 2) but the 95^{th} percentile and maximum values indicate that very large fires occur at higher wind speeds too.

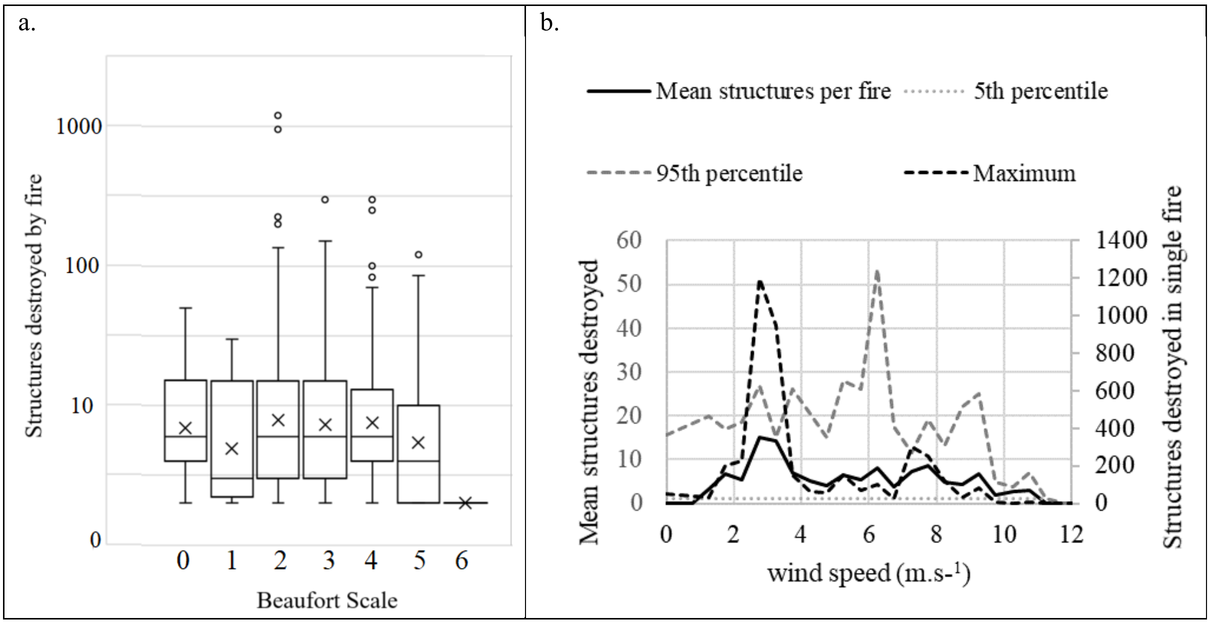

Figure 8. a. Box-and-whisker graph of number of structures destroyed (Cape Town Fire Incidence database) in individual fires at each wind category (SAWS data). Note the use of a log scale on the y-axis and b. Structures destroyed in fires at full range of wind speeds showing mean structures per fire on the primary vertical axis, and 5^{th} percentile, 95^{th} percentile and maximum number of structures destroyed in a single fire on the secondary vertical axis.

The count and probability of fires starting and spreading under different wind conditions are illustrated in Figure 9. The data is analysed at three levels: wind conditions for all fires, wind conditions for fires which spread beyond the dwelling of origin (representing 33% of the sample) and fires which destroyed at least ten dwellings (the 90^{th} percentile). These are the criteria used in the analysis shown in Figure 9 but first the count of each wind condition is shown for comparative purposes (Figure 9a). The different criteria are shown in the rows with number of occurrences displayed in the “Count” column and the probability of fires occurring is displayed in the “Probability”.

Figure 9b shows that fires predominantly start under prevailing wind conditions however the probability of fires starting (Figure 9c) is highest when wind blows from the SSW at speeds of 7 $m.s^{-1}$ (Beaufort Scale 4) with a 20% probability of fire occurring in the hour with those conditions. A second peak in probability (12.5% probability) is when the wind blows from the ESE at 9 - 10 $m.s^{-1}$ (Beaufort Scale 5). The highest count of fires spreading beyond the dwelling of origin (Figure 9d) occurs when the wind blows from SSE at a speed of just below 5 $m.s^{-1}$ (Beaufort Scale 3), however the probability of these fires occurring (Figure 9e) is highest (12.5% probability) when the wind blows from ESE at higher speeds of around 10 $m.s^{-1}$ (Beaufort Scale 5). The wind conditions for the number of fires destroying at least ten dwellings (Figure 9f) is similar to that of fires which spread beyond the dwelling of origin (Figure 9d), but the probability of fires destroying at least ten dwellings is more distributed with respect to direction, and wind speeds tend to be lower, ranging from approximately 3 to 8 $m.s^{-1}$ (Beaufort Scale

3 and 4) and the probability of these occurring in the hour with these conditions being much lower and not exceeding 2%.

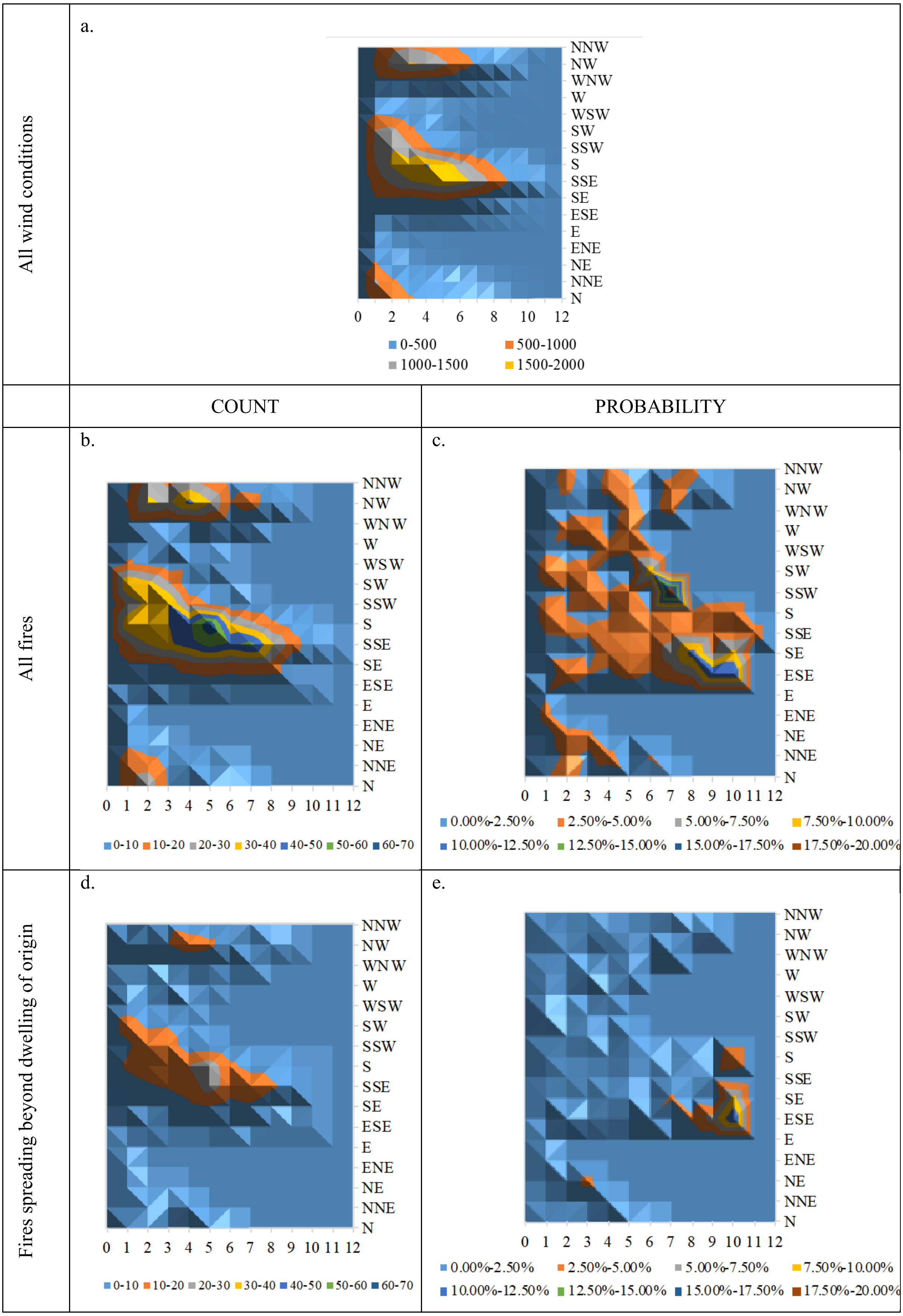

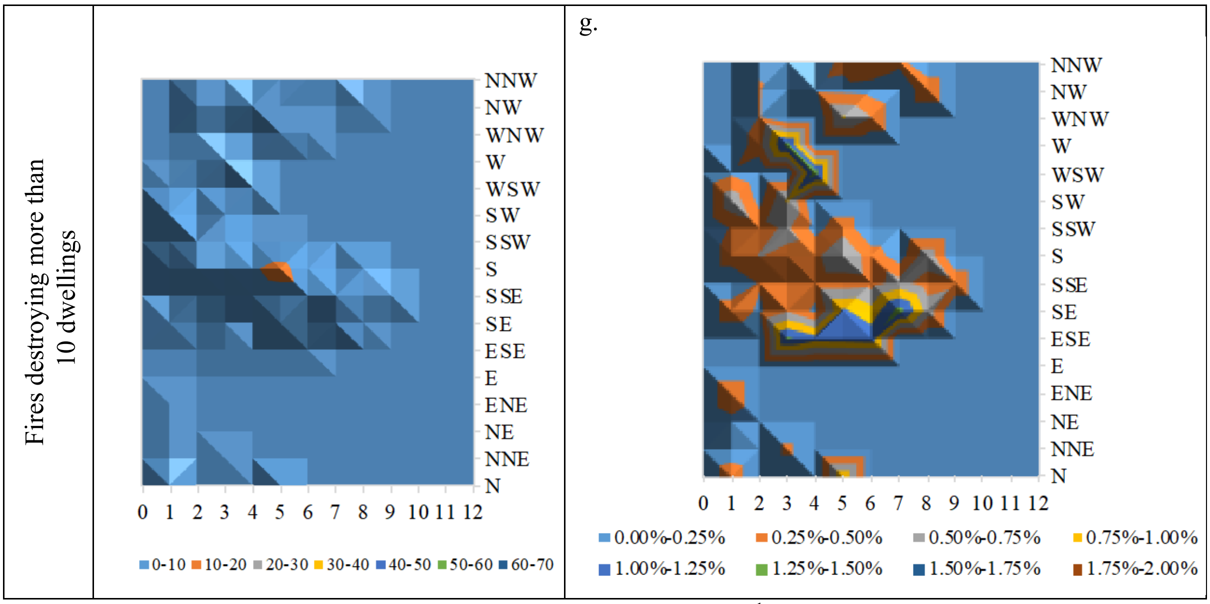

Figure 9. Wind conditions (direction on y axis and speed in m.s^{-1} on x axis) under which fires occur (count) and the probability of fires occurring and the size of the resulting fire. a. Count of all wind conditions, b. Count of wind conditions for all fires, c. Probability of wind conditions for all fires, d. Count of wind conditions for fires spreading beyond dwelling of origin, e. Probability of wind conditions for fires spreading beyond the dwelling of origin, f. Count of wind conditions for fires destroying more than ten dwellings, and g. Probability of wind conditions for fires destroying more than ten dwellings (note scale is order of magnitude less than previous probability plots in 9c, and 9e).

Fires mapped using remote sensing

The final dataset [20] of the confirmed Fire Extent Areas contains 46 polygons ranging in date from 17 May 2014 to 21 November 2018. Analysis of the Fire Extent Areas with respect to number of fire incidents, size of the fire and the month of fire incident (Figure 10) reveals a similar trend to that obtained from the Fire Incidence data. The majority of fires occurred from October to December, three of the windiest months in Cape Town and the total area burned was highest in October and November. The winter months recorded both low number of fire incidents (Figure 10.a) and a lower Fire Extent Area (Figure 10.b).

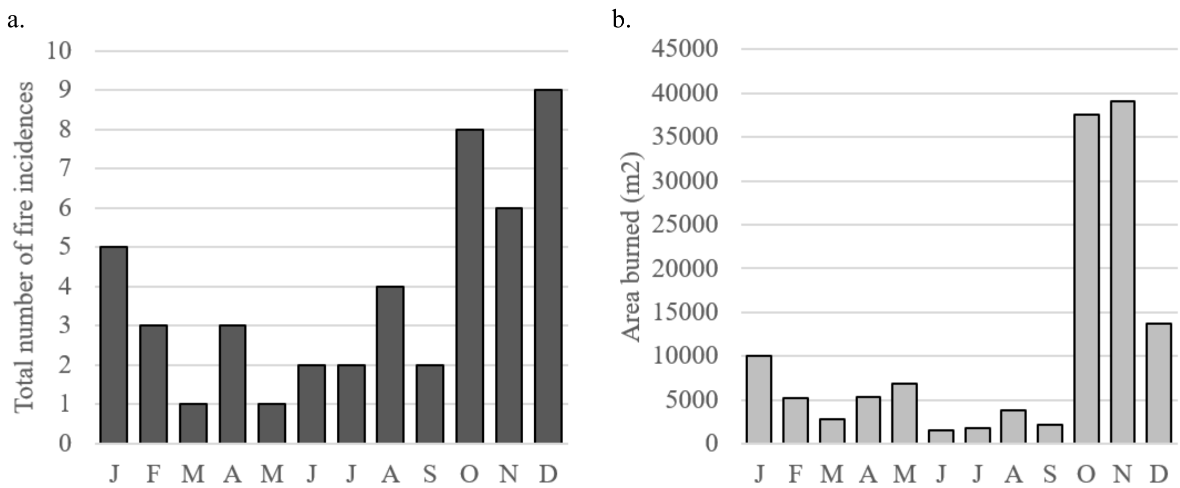

Figure 10.a. Number of fire incidents and b. Total Fire Extent Area (sum) by month from the historic fires mapped using remote sensing

Since it is possible that the remote sensing method of mapping fires did not detect all fires which may have occurred and thus the full range and distribution of fire size may not be present in this dataset, some measure is required to determine if the statistical distribution of the Fire Extent Areas is fit for comparison with the GUA ("Potential Fire Areas"). The Fire Extent Areas ranged in size from 345 m^2 to 27894 m^2 (Table 1) and it can therefore be assumed that the minimum size of a fire which can be detected using the remote sensing method is 345 m^2. For this reason, all polygons in the "Potential fire area" dataset which are less than 345 m^2 in area are removed from the analysis. This resulted in 1278 polygons for the City of Cape Town representing Potential Fire Areas ranging in size from 345 m^2 to 114 048 m^2.

The histograms for the Fire Extent Areas (Figure 11.a) and Potential Fire Areas (Figure 11.b) and descriptive statistics (Table 1) reveal a high positive kurtosis (Leptokurtic distribution) of Potential Fire Areas indicating a high probability of either extremely small or extremely large fires and although the kurtosis is also high (23) for Fire Extent Areas, it is significantly lower than the kurtosis for Potential Fire Areas (71.6). This implies that the Fire Extent Areas do not reflect the full range in size of potential fires, particularly with respect to larger areas (as shown by the larger positive skewness value for potential fire areas compared with actual fires). This could be due to fire suppression intervention which decreases the extent of an actual fire compared with its potential extent in the absence of fire suppression.

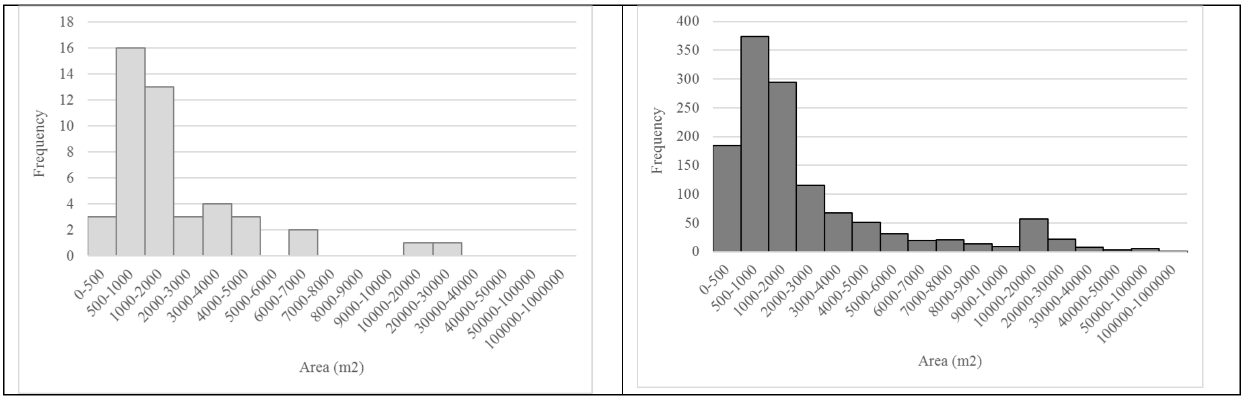

Figure 11. Histogram showing frequency distribution of a. Fire Extent Areas and b. Potential Fire Areas.

Table 1. Descriptive statistics (m^2) of Fire Extent Areas and Potential Fire Areas

Descriptive statistics	Fire Extent Areas	Potential Fire Areas
Mean	2655	3396
Median	1389	1165
Standard Deviation	4502	7329
Kurtosis	23.0	71.6
Skewness	4.5	6.9
Range	27548	113702
Minimum	345	345
Maximum	27894	114049
Count	46	1278

Spatial metrics

Descriptive statistics for each spatial metric for the 46 Fire Extent Areas are compared with the 1278 Potential Fire Areas in Table 2.

Table 2. Descriptive statistics of spatial metrics for Fire Extent Areas and (Potential Fire Areas)

Descriptive statistics	PLAND Density,%	Average ENN, m	Standard deviation ENN, m	ED, m/ha
Mean	81.5 (83.4)	0.34 (0.66)	0.21 (0.45)	5241 (5440)
Median	80.3 (83.0)	0.33 (0.62)	0.18 (0.44)	5381 (5456)
Standard Deviation	7.4 (4.2)	0.10 (0.27)	0.13 (0.18)	641 (721)
Kurtosis	1.2 (1.0)	0.07 (3.9)	3.25 (1.55)	-0.92 (1.55)
Skewness	-0.63 (0.6)	0.58 (1.39)	1.46 (0.69)	-0.12 (-0.43)
Range	37.0 (28.8)	0.41 (2.12)	0.65 (1.45)	2404 (6356)
Minimum	59.9 (70.3)	0.18 (0.19)	0.03 (0.01)	4058 (1933)
Maximum	96.9 (99.0)	0.59 (2.31)	0.68 (1.46)	6462 (8289)

Analysis (Table 2) of the dwelling density for the Fire Extent Areas reveal generally high dwelling density ranging from 60.0% to 96.9% with a mean of 81.5% (median 80.3%). However when compared with the Potential Fire Areas, the dwelling density is lower for the Fire Extent Areas compared to the majority of Potential Fire Areas (min 70.3%, max 99.0%, mean 83.2%). Further the kurtosis and skewness of the two datasets reveal that the density of the Potential Fire Areas dataset is normally distributed with it being marginally skewed in the direction of high densities. The density of the Fire Extent Areas dataset reveals a skewness in the opposite direction with the probabilities of lower densities being higher than in the potential fire dataset. This may indicate that real fires regularly exceed the recommended safe critical separation distance of 3 m (note that the 3 m safe separation distance estimated by previous researches did not account for wind effect) – the distance used to create the Potential Fire Area dataset, or it may be an indication that the method to create the Potential Fire Areas is biased towards creating polygons with a high dwelling density as the polygon does not include all gaps between connected dwellings, only those gaps which are less than 3 m.

For the average Euclidian nearest neighbour (ENN) calculation (Table 2), ENN distances of less than 10 cm are removed and a merged dwelling is assumed. Since the spatial resolution of the aerial photography is 6 cm (one pixel equals 6 x 6 cm on the ground), a higher precision of measurement becomes meaningless. The results of the average ENN for the Fire Extent Areas reveal lower values for the first nearest neighbours (average 0.34 m) when compared with the Potential Fire Areas (0.66 m)

Cumulative probability densities of the first, second and third ENN (Figure 12) show that for the first, second and third nearest neighbours, the probability of the distance between neighbours is most likely to be the smallest in the Fire Extent Areas dataset, followed by the Potential Fire Areas dataset and finally all informal dwellings dataset. This demonstrates that the nearest neighbour is an important parameter in contributing towards fire spread and it is not only the first nearest neighbour which plays a role but also second and third neighbours - likely demonstrating a more dense settlement.

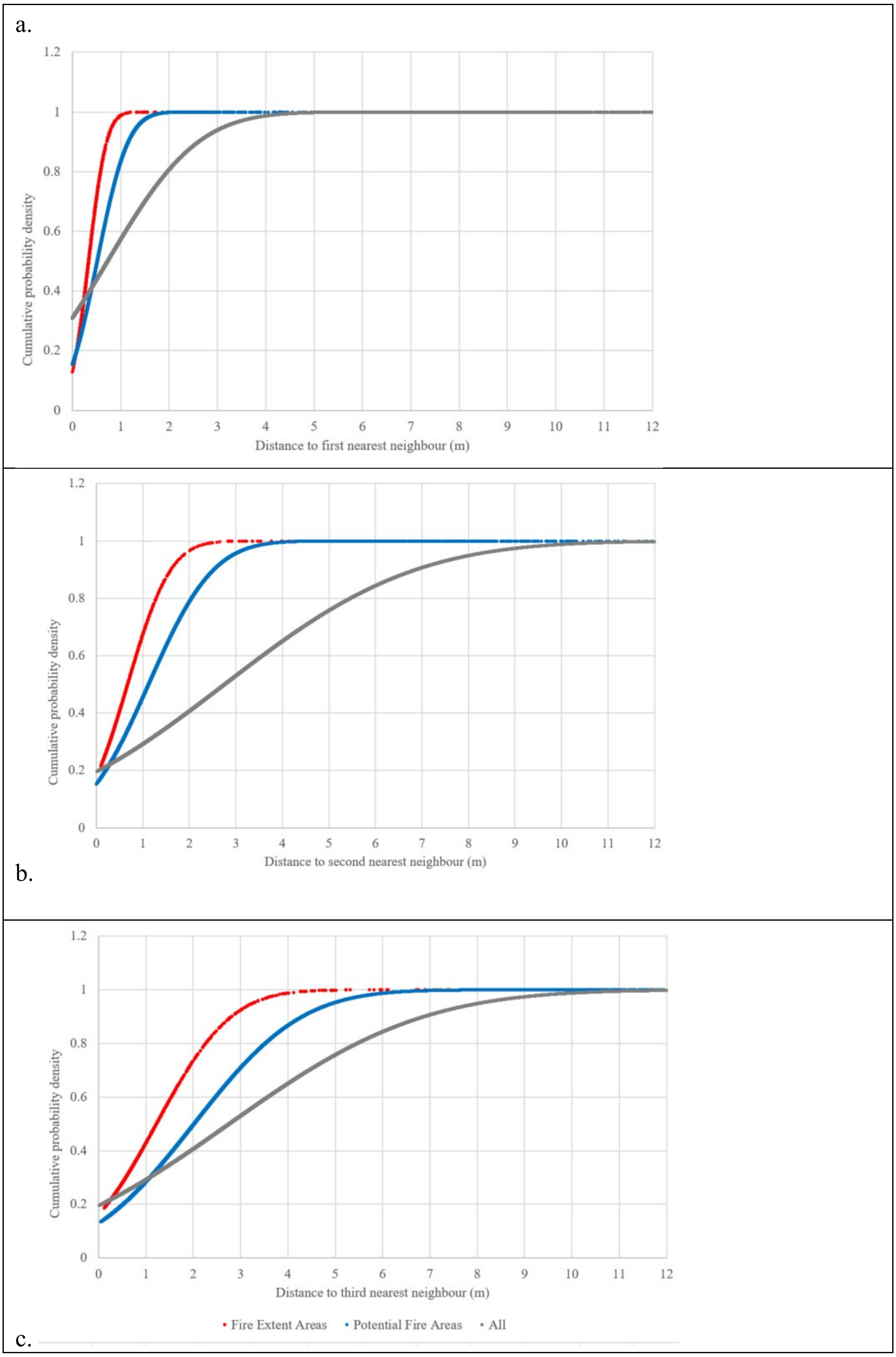

Figure 12. Cumulative probability densities of distance to a. first, b. second, and c. third nearest neighbours for Fire Extent Areas, Potential Fire Areas and All (all dwellings in informal dwelling footprints layer, including those which fall in FEAs and PFAs).

The results of the analysis of distance to first ENN against the range in distance from first to third ENN is shown in Figure 13 for All dwellings in informal settlements in Cape Town, Potential Fire Areas and the Fire Extent Areas. Again, it should be noted that the precision of the data is considered to be 0.1 m and therefore measurements of less than 0.1 m are assumed to equal zero. It is apparent that both distance to first nearest neighbour and the range is smallest for the Fire Extent Areas, followed by the Potential Fire Areas and then All dwellings. This confirms the findings that dwellings in the Fire Extent Areas are constructed closer together than is typical across the rest of informal settlements in the City of Cape Town. The use of the buffering distance in creating the PFAs can be seen in the abrupt limit of the PFAs in Figure 13.

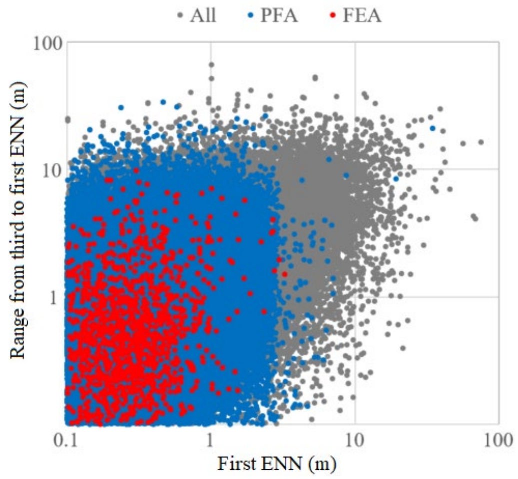

Figure 13. Scatterplot of distance to first ENN (x-axis) against range in distance from first to third nearest neighbour (y-axis) for the Fire Extent Areas, the Potential Fire Areas and All dwellings in Cape Town's informal settlements.

The range of edge density (ED) values for the Fire Extent Areas is smaller than the Potential Fire Areas (Table 2) demonstrating that the edge density of Potential Fire Areas is more widely distributed (higher kurtosis) than in Fire Extent Areas.

Thresholding spatial metrics

A lower average ENN and standard deviation of ENN was found for the Fire Extent Areas when compared with the Potential Fire Areas. Contrary to generalised statement around density [8,9] the dwelling density does not appear to be a good indicator of fire spread risk, but edge density in the Fire Extent Areas covers a smaller range than in the Potential Fire Areas. It has also been stated [19] that combining spatial metrics may give more insight into fire spread risk than considering spatial metrics separately. On this basis, intermediate ED, low average ENN and low standard deviation of ENN indicate large dwellings consistently close together. The threshold values of these three spatial metrics are obtained by selecting the 75th percentile value for the Fire Extent Areas and these values - average ENN (0.39 m), standard deviation ENN (0.26 m), and for ED the interquartile range (4443 – 5161 m/ha) - are applied to the Potential Fire Areas dataset to highlight those areas which fulfil all three spatial metric criteria. The use of the 75th percentile ensures that the top quartile of average ENN and standard deviation ENN are retained. A higher threshold could have been selected, such as the 95th percentile, however since only the Potential Fire Areas which meet all three threshold values are retained, a higher threshold could lead to only outliers being retained. Applying these thresholds to the 1278 Potential Fire Areas, only 37 meet the high fire spread risk criteria.

The largest ten Potential Fire Areas meeting the threshold conditions are identified and shown in Table 3 and Figure 2. Two of the largest ten Potential Fire Areas fall within the Greater Khayelitsha area, three within Kosovo, with the known fire hotspots of Philippi, Masiphumelele, Imizamo Yethu and Doornbach also represented. Interestingly, all of the top ten largest Potential Fire Areas on the basis of these metrics have a dwelling density below the mean dwelling density for Potential Fire Areas (83.4%, see Table 1). It can also be seen that although the average ENN threshold is set at 0.39 m (for the whole of Cape Town), the highest value in the top ten (Table 3) is 0.34 m implying that the threshold values for standard deviation ENN, and ED restrict the average ENN below the threshold value. This reinforces the importance of using more than one spatial metric as relying on one metric alone only captures a single aspect of fire risk within a settlement.

Table 3. Ten largest Potential Fire Areas meeting the ENN and ED threshold criteria.

ID	Settlement	Potential fire size, (m^2	Average ENN, m	Standard Deviation ENN, m	Density, %	ED, m/ha
324	Kosovo	78 341	0.29	0.22	79.67	5 144
597	Victoria Mxenge Khayelitsha	32 192	0.34	0.25	82.63	4 653
744	Masiphumelele	30 046	0.34	0.26	80.58	4 651
1198	Block 6 Philippi	21 605	0.33	0.23	80.60	5 119
599	Victoria Mxenge Khayelitsha	20 172	0.34	0.25	81.28	4 475
556	Doornbach (Dunoon)	16 866	0.27	0.19	80.09	4 826
335	Kosovo	11 733	0.30	0.20	80.76	5 075
908	Phola Park - Gugulethu	11 524	0.32	0.23	80.66	4 894
808	YMCA – Imizamo Yethu	9 312	0.32	0.18	82.95	4 968
347	Kosovo	8 666	0.29	0.25	81.82	4 851

Thresholding of the analysis of the distance to first ENN against the range from first to third ENN using the 75th percentile value of both variables, allows for the identification of particular dwellings which are at risk of fire spread. It should however be noted that these threshold values were obtained from the 46 Fire Extent Areas obtained and therefore the inclusion of additional fires into the data may change the threshold values. Thus, the dwellings not identified being at risk using this method cannot necessarily be described as immune from fire spread risk, however they are likely less at risk than the identified at-risk dwellings. The 75th percentile values are 0.38 m and 0.90 m for distance to first ENN and range respectively. The ENN 75th percentile value differs very slightly from the 0.39 m value reported above as if a dwelling with fewer than three nearest neighbours were excluded from this part of the analysis. This dataset is presented as a kmz in the supplementary information where TRUE equals a dwelling at risk of fire spread using the threshold method and FALSE does not.

By way of example, using the results of settlements at risk in Table 3, maps (Figure 14) of the broader Kosovo settlement (Figure 14.a), Victoria Mxenge (Figure 14.b) and Masiphumelele (Figure 14.d) are displayed to illustrate high risk settlements, with the settlement of Klipfontein Glebe (Figure 14.c) selected as being representative of a more dispersed settlement [21]. In Figure 14 it can be seen that almost all dwellings in Kosovo are at risk of fire spread, whereas in Victoria Mxenge the narrow sections of the settlement contain dwellings least at risk – likely because they have fewer than three nearest neighbours. Klipfontein Glebe is largely dispersed and not at risk, however there are clusters of dwellings within the settlement which are at risk, particularly in the south. The outlines for known fires in Masiphumelele [22] are overlaid on the dwelling at risk map (Figure 14.d) demonstrating that this settlement has indeed been impacted by large fires with the largest fires occurring on 2 May 2011 and 29 November 2015 in wind conditions: direction and speed of NW, 2.8 $m.s^{-1}$ and SSW, 3.1 $m.s^{-1}$ respectively. The other fires which could be found in the fire incident database have their wind conditions and structures destroyed listed here: 14 January 2014, 27 structures destroyed, wind from SW at 1.2 $m.s^{-1}$; 23 May 2014, 225 structures destroyed, wind from S at 2.2 $m.s^{-1}$; 1 May 2015, 16 structures destroyed, no wind. It should however be noted that the dwelling outlines displayed in Figure 14 were captured from aerial photography dated February 2018 so the dwellings at risk are correct at that date. However, due to the fires, the dwelling outlines may have changed slightly, representing a slightly different risk at the time of the fire.

Figure 14. Dwellings at risk of fire spread in a. Kosovo, b. Victoria Mxenge, c. Klipfontien Glebe and d. Masiphumelele.

Discussion

From this research it has been shown that density alone is not a good predictor of fire severity, supporting the finding of early research [23]. In that research, although the metrics for dwelling density differed to PLAND used in this paper, it was found that the settlements of Imizamo Yethu and Joe Slovo both had areas which experienced high fire severity yet had only average to below average densities.

The use of the first three ENNs allows for the identification of particular dwellings which are at risk of fire spread by using a threshold approach combining both first ENN and the range from first ENN to third ENN. This approach allows both for identification of dwellings at risk within settlements which were not identified as being high risk (such as Klipfontein Glebe) and also to give an idea of the proportion of dwellings at risk within the identified high risk settlements.

Concerning how wind will affect fire spread through a settlement, it is important to understand how wind affects the compartment fire dynamics, particularly the heat transfer from one dwelling to another, as well as the possible flame impingement that occurs from flame plumes ejected at compartment openings. Past studies have examined features of these plumes such as the heat flux to the wall above the opening and the temperature of the gases within the plume (e.g. [24]). In the informal settlement context, fire spread is from dwelling to dwelling, so it is key to understand the spatial position of the plume and heat transfer from the flame plume and the opening relative to an adjacent dwelling.

The deflection of the flame plume as a result of wind can be described in simple terms. As the wind speed increases, both the vertical flame height and the distance between the flame tip and the target dwelling decrease, as depicted in Figure 15. The change of flame shape and position will change the configuration factor involved in radiative heat transfer, as will be discussed, and the extension of the flame will increase the probability of flame impingement at an adjacent dwelling.

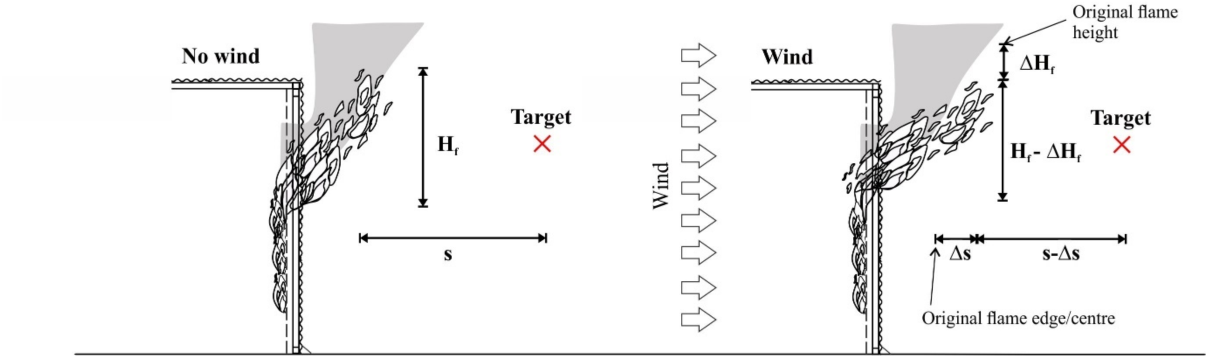

Figure 15. Visual illustration of how the flame height (H_f) and flame-target separation distance (s) change in the presence of wind.

Correlations have been developed for estimating the position of the fire plume under no-wind and wind conditions. Many current methods (e.g [25–27]) are adapted versions of the well-known method of Law and O'Brien [28]. Using the method in EN 1991-1-2:2002 [29], the horizontal projected flame length (L_h) and vertical height above the opening (L_v) can be calculated from equations B.7 and B.8 in no-wind conditions and B.20 and B.21 with wind. For three example square openings of side length 0.8m, 1m and 1.2m, these dimensions were calculated (Figure 16). It was assumed that the heat release rate ($\dot{Q}$) of the compartment is 3.5MW, which is comparable to experimental values from [30], with a total ventilation area (A_v) of $2.5m^2$.

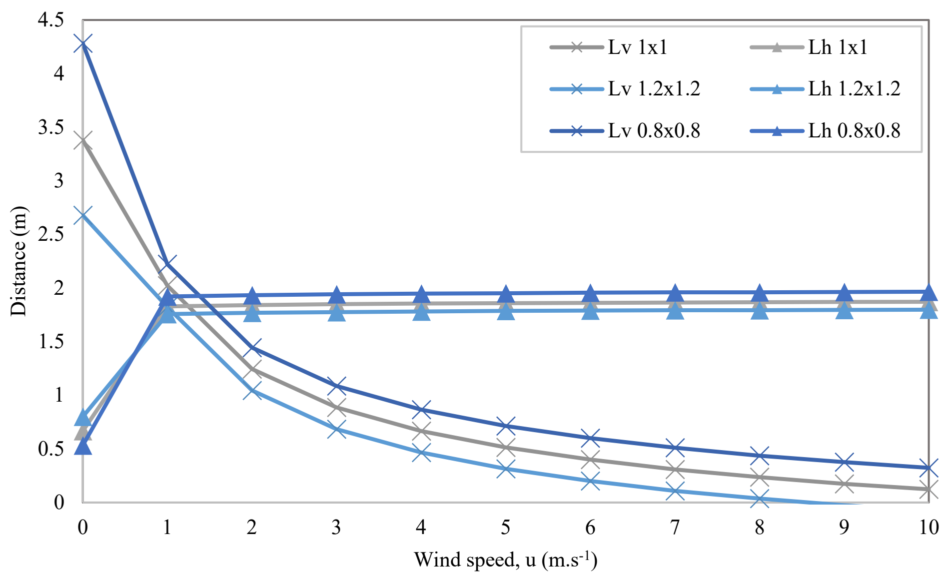

Figure 16. External flame dimensions for different square openings as calculated by EN 1991-1-2:2002

Clearly, even under low wind speeds, the horizontal projection of the flame is expected to increase substantially from 0.5-0.8 m to 1.8-2.0 m. This will significantly increase the probability of flame impingement between dwellings. Referring back to Figure 12, this suggests that across all dwellings in the study area, the proportion of 1st ENNs within the equivalent distance to horizontal flame length rises from approximately 50% to 80%. For both 2nd and 3rd ENNs, this increase is in the region of 25% to 40%. This analysis also implies that virtually all 1st ENNs across the identified PFAs lie within the calculated flame length under wind conditions. That is not to assume that all ENNs lie adjacent to an opening on a neighbouring dwelling, but for those which do, the proportion that lie within the flame impingement distance should increase comparably under wind conditions.

However, from Figure 8 it is apparent that there is no notable increase in fire size from Beaufort Scale 0 to 1 (0-0.5 $m.s^{-1}$ to 0.6-1.5 $m.s^{-1}$). It is proposed that [28] and subsequent models overestimate the flame length at lower wind speeds. Certainly, in other studies [25,31] it is apparent that the projection of the plume is more gradual than is implied in this model [28] when the wind speed rises above zero. Therefore, the method overestimates the horizontal projection of flame at low wind speeds. This error is also apparent in the following analysis of radiation from the plume and opening.

From Figure 8, the number of dwellings destroyed by fire starts to decrease as the wind speed surpasses a Beaufort Scale of 4 (approximately 5.6-7.9 $m.s^{-1}$) and confirmed in Figure 9.g, where it can be seen that the probability of large fires decreases after a wind speed of approximately 8 $m.s^{-1}$. The authors postulate that this behaviour is as a result of a flame height tending to a minimum at increasing wind speeds whilst the horizontal projection tends to a maximum (i.e. the flame tilt angle tends to a maximum). In other words, the angle between the vertical line from the centre of a burning item (the window of the burning dwelling in this case) to the intersection of the wind-tilted flame axis has a limit. The radiation received at a given point from the flames ejecting out of a window of a burning dwelling can be described by the following equation [32]:

$$\dot{q}''_{inc} = \sigma \emptyset \varepsilon_f T_f^4 \quad (1)$$

where σ is the Stefan-Boltzmann constant (5.67×10^{-11} kW/(m^2 K^4)); $\emptyset$ is the configuration factor between the flame and the receiver's surfaces, ε is the emissivity of the flame; and T is the temperature (K) of the flame. The configuration factor can be calculated as follows [32]:

$$\emptyset = \int_0^{A_f} \frac{\cos\theta_f \cos\theta_T}{\pi s^2} \cdot dA_f \quad (2)$$

where A_f is the area of the flame's surface emitting heat to the target dwelling and θ_f (and θ_T) is the angle between the surface normal $\hat{n}f$ (and $\hat{n}_T$) and the line connecting dA_f to dA_T (of length s).

Several mathematical models have been applied to develop on these numerical principles of radiation and evaluate the radiative heat flux at a distance from a compartment opening which is ejecting a flame. Each model presents slightly different methods for conceptualising the shape of the flame to enable calculation of the configuration factor(s). These models have been tested and compared against experimental data [33]. However, it does not appear any of these methods have yet been adapted to account for the effects of wind. Using the method of Chen and Francis [25], and inputting corrected flame lengths, heights and widths as per the previous calculations (see eqns. B.20-22 in [29]) the wind-varying radiative heat flux at various lateral distances from the centre of the upper edge of a window can be evaluated (Figure 17). The calculations assume an opening of 1×1m, a plume gas emissivity of 0.519 [26], and a flame temperature at the opening of 1150K [15]. The lateral distances shown in Figure 17 were selected as they lie at or outside of the approximate 2 m flame impingement distance. This analysis shows that the deflection of a fire plume as a result of wind, not only increases the risk of flame impingement, but can increase heat fluxes in the further field above the critical heat fluxes (CHF) for materials that may be found in informal settlements [34]. However, as wind speeds approach and exceed 10 $m.s^{-1}$ the shortening of the vertical flame height as a result of the wind causes reductions in heat flux back to levels comparable with no wind conditions, perhaps correlating to the reduction of fire size over Beaufort Scale 4 to 6 (Figure 8). There is a significant initial spike in heat flux from 0 to 1 m.s^{-1} which is again likely indicative of the conservative evaluation of horizontal flame projection at low wind speeds implicit within [28]. With the exception of this proposed error, the analysis provides a reasonable comparison with evidence from the fire incidence data (Figure 8a): wind has a maximal effect on fire spread at speeds of 1.6-3.3 m.s^{-1} (Beaufort 2), but at faster wind speeds actually starts to reduce the risk of spread relative to this maximum.

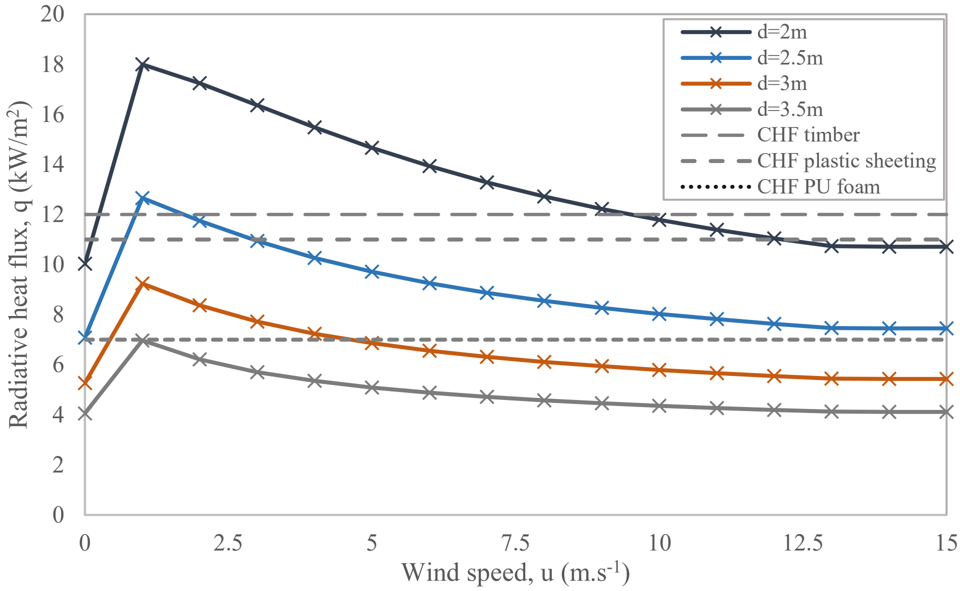

Figure 17. Radiative heat flux at different opening-dwelling separation distances (d), showing CHFs for selected materials as per [34]

The effect of the wind on the flame plume appears to be twofold in that it 1) extends the distance over which possible flame impingement, and subsequent ignition can occur, and 2) increases the radiative heat flux in the further field above critical values for ignition for some common materials in informal settlements. However, this analysis is far from complete and it is suggested that the effects of wind on compartment fire dynamics – particularly the lateral deflection of external plumes – should be a focus of further research given the current lack of studies on the subject. Small scale experiments have revealed that wind may increase the heat release rate of a compartment [35] – which will theoretically increase the projected flame height – and the gas temperature at openings [36], but robust correlations have not yet been developed for such tests or validated for applicability at full-scale. Such future advances in knowledge should be used to update the analyses laid out above. Consideration must also be made for multiple dwellings burning adjacent to each other: in experimental work [37] flame heights of up to 3 m above the openings were recorded at wind speeds in excess of 10 km.h^{-1} (2.8 m.s^{-1}), over double the heights predicted in Figure 16.

In addition to the deflection of external flames, the overall rate of fire spread in a settlement is also related to wind-dependant compartment fire growth. In the case of thermally thick compartments where convective losses are minimal, higher wind speeds increase the oxygen supply so reduce the time to flashover and increase the peak heat release rate of the fire [35]. However, for thermally thin compartments, where the walls are rapidly thermally penetrated, convective heat losses are more influential. Faster winds increase the heat release rate required to initiate flashover in the compartment (HRR_{fo}) [3], potentially delaying or even preventing flashover. The impact of wind on a single dwelling is therefore duplicitous in nature, having the potential to increase the time required to reach flashover but then decrease the time to spread to the next dwelling. Once the fire has spread beyond the origin dwelling to several others, the impact of these phenomena are less clear, with the wind clearly driving fast rates of spread in large conflagrations [5,37]. Nevertheless, the overall effect of high winds delaying or preventing flashover is consistent with the finding that larger fires have tended to occur at light and moderate wind speeds (1.6-7.9 $m.s^{-1}$) rather than higher wind speeds (>7.9 $m.s^{-1}$) (Figure 8).

It can be challenging to make direct comparisons between this work and other studies since the data resolution and metrics that are mapped vary. In the wider urban context it is rare that fire risk is mapped to individual buildings or dwellings. Many studies present mapped risk to the resolution of districts or neighbourhoods – this is the case for both physics-based fire spread models [38] and risk-metric models [39–41]. Where fire risk has been mapped at the resolution of individual buildings in formal contexts, such as [42], the concept of risk neglects risk of spread between buildings and only focuses on in-building risk factors.

Where dynamic fire spread models have been applied they may have the advantage of producing relative risk distributions across individual buildings at the cost of being computationally heavy [43], or map risk at a cellular-, rather than individual building-, level [44]. Therefore, the approach laid out in this paper is comparably a novel and effective method to use as a quick evaluation of risk, relying on relatively fewer metrics. It can also swiftly outline the inherent risk status of thousands of informal dwellings independent of a specific fire event.

Finally, the possibility that the wind speeds and directions recorded at the weather station are not fully representative of all locations in Cape Town must be considered. The ideal scenario would be to have hourly wind data collected for a multitude of locations in close proximity to informal settlements. Future research could include the installation of a weather station within or on the boundary of settlements such as Masiphumelele which experience frequent and large fires.

Conclusion

This paper explored the effect of wind speed and direction on the size of fires of Cape Town's informal settlements using a) Fire Incidence data collected by the City of Cape Town and b) fires identified using Sentinel-2 satellite imagery (Fire Extent Areas). Spatial metrics calculated using dwelling footprints captured from very high resolution aerial photography were analysed for the Fire Extent Areas to determine threshold values at which fire spread was likely to occur. To identify areas at risk of fire spread, a geographical unit of analysis was created using a safe critical separation distance of 3 m where dwellings within 3 m of each other were considered to belong to the same Potential Fire Area. Threshold values for spatial metrics of average nearest neighbour, standard deviation of nearest neighbour and edge density obtained from the Fire Extent Areas were applied to the Potential Fire Areas to identify the largest informal settlement areas in Cape Town at high risk of fire spread.

The results showed that larger fires are generally associated with medium winds and large fires generally occur at the windy times of year but beyond a wind speed of approximately 8 $m.s^{-1}$ large fires are less frequent. It is postulated that this is because above these speeds, the wind will not decrease the distance between the flame and adjacent dwelling any further, but the reduction in flame height will reduce the radiation to neighbouring dwellings. Additionally, higher wind speeds are associated with higher convective heat transfer coefficients, implying that convective cooling would have an increasing effect, increasing time-to-ignition and flashover of the next dwelling. Yet this should be treated with caution, since if a fire does manage to establish beyond the origin dwelling, moderate and strong winds can still drive large conflagrations to an extent that would not occur in the absence of wind. Additionally, current methods for assessing heat fluxes outside of a burning dwelling require future work to strengthen the analyses laid out in this paper. Some of these findings, such as the effect of the wind speed on flame length and radiative heat transfer, can be applied to settlements in other locations around the world. Other factors are likely to be geography specific such as the probability of fire occurring in certain wind conditions as this is a function of prevailing wind conditions in a location.

With respect to spatial metrics, it was found that dwelling density on its own is not a good predictor of fire spread risk, perhaps due to the method used to determine the Potential Fire Areas rather than the metric itself being unsuitable. It was however found that average nearest neighbour, standard deviation of nearest neighbour and edge density can be used in combination to identify areas at risk of fire spread, with edge density being the least important of the three metrics. Low values of these three metrics together possibly indicate large dwellings in consistent close proximity to each other. A threshold approach using the distance from a dwelling's first nearest neighbour together with the range in distance from the dwelling's first to third nearest neighbours allow for the identification of specific dwellings within a settlement which are at risk of fire spread.

Although this paper has relied on large datasets from multiple sources, the detail in the data has led to only tentative conclusions being drawn. However, since the scientific study of informal settlement fires is relatively new, this paper represents new knowledge and highlights the possibilities of using spatial metrics and wind speed and direction for fire spread risk identification.

Acknowledgements

This research was funded by IRIS-Fire project of UK (Engineering and Physical Sciences Research Council Grant no.: EP/P029582/1).

References

1. Rush, D.; Bankoff, G.; Cooper-Knock, S.-J.; Gibson, L.; Hirst, L.; Jordan, S.; Spinardi, G.; Twigg, J.; Walls, R. Fire risk reduction on the margins of an urbanizing world. *Disaster Prev. Manag. An Int. J.* 2020, *ahead-of-p*.

2. Gqirana, T. Cape Town is the fire capital of South Africa Available online: https://www.news24.com/SouthAfrica/News/cape-town-is-the-fire-capital-of-sa-20151208 (accessed on May 6, 2020).

3. Centeno, F.; Beshir, M.; Rush, D. Influence of the wind on the likelihood to flashover within thermally-thin small-scale compartments. *Unpubl. Manuscr.* **2019**.

4. Wang, Y.; Gibson, L.; Beshir, M.; Rush, D. Preliminary Investigation of Critical Separation Distance Between Shacks in Informal Settlements Fire BT - The Proceedings of 11th Asia-Oceania Symposium on Fire Science and Technology. In; Wu, G.-Y., Tsai, K.-C., Chow, W. K., Eds.; Springer Singapore: Singapore, 2020; pp. 379–389.

5. Kahanji, C.; Walls, R. S.; Cicione, A. Fire spread analysis for the 2017 Imizamo Yethu informal settlement conflagration in South Africa. *Int. J. Disaster Risk Reduct.* **2019**, 101146, doi:10.1016/J.IJDRR.2019.101146.

6. Walls, R.; Olivier, G.; Eksteen, R. Informal settlement fires in South Africa: Fire engineering overview and full-scale tests on "shacks." *Fire Saf. J.* **2017**, *91*, 997–1006, doi:https://doi.org/10.1016/j.firesaf.2017.03.061.

7. Herold, M.; Liu, X.; Clarke, K. Spatial Metrics and Image Texture for Mapping Urban Land Use. *Photogramm. Eng. Remote Sens.* **2003**, *69*, 991–1001.

8. Walls, R. S.; Zweig, P. Towards sustainable slums: understanding fire engineering in informal settlements. In *Advanced Technologies for Sustainable Systems*; 2017; pp. 93–98.

9. Twigg, J.; Christie, N.; Haworth, J.; Osuteye, E.; Skarlatidou, A. Improved Methods for Fire Risk Assessment in Low-Income and Informal Settlements. *Int. J. Environ. Res. Public Heal.* 2017, *14*.

10. City of Cape Town Fire incidence data Available online: https://web1.capetown.gov.za/web1/opendataportal/DatasetDetail?DatasetName=Fire incidence.

11. Gibson, L.; Engelbrecht, J.; Rush, D. Detecting historic informal settlement fires with sentinel 1 and 2 satellite data - Two case studies in Cape Town. *Fire Saf. J.* **2019**, doi:10.1016/j.firesaf.2019.102828.

12. City of Cape Town Open Data Portal - Data Set Description: Aerial photography 2015 - 2018. Available online: https://web1.capetown.gov.za/web1/opendataportal/DatasetDetail?DatasetName=Aerial photography (accessed on Aug 27, 2019).

13. University of Edinburgh. School of Engineering. Infrastructure and Environment. Dwelling outline - Informal Settlements of Cape Town, 2018 [dataset]. 2020.

14. Stevens, S.; Gibson, L.; Rush, D. Conceptualising a GIS-based risk quantification framework for fire spread in informal settlements: A Cape Town case study. *Int. J. Disaster Risk Reduct.*

15. Cicione, A.; Walls, R. S.; Kahanji, C. Experimental study of fire spread between multiple full scale informal settlement dwellings. *Fire Saf. J.* **2019**, *105*, 19–27, doi:10.1016/J.FIRESAF.2019.02.001.

16. Cicione, A.; Beshir, M.; Walls, R. S.; Rush, D. Full-Scale Informal Settlement Dwelling Fire Experiments and Development of Numerical Models. *Fire Technol.* **2019**, doi:10.1007/s10694-019-00894-w.

17. Cicione, A.; Walls, R.; Sander, Z.; Flores Quiroz, N.; Narayanan, V.; Stevens, S.; Rush, D. The effect of separation distance between informal dwellings on fire spread rates based on experimental data and analytical equations. *Fire Technol.* **2020**.

18. Wang, Y.; Gibson, L.; Beshir, M.; Rush, D. Preliminary investigation of critical separation distance between shacks in informal settlements fire. In *The 11th Asia-Oceania Symposium on Fire Science and Technology*; 2018.

19. Gibson, L.; Adeleke, A.; Hadden, R.; Rush, D. Spatial metrics from LiDAR roof mapping for fire spread risk assessment of informal settlements in Cape Town, South Africa. *Fire Saf. J.*

20. Gibson, L. Fire in Cape Town informal settlements mapped from remote sensing, 2014-2018. Available online: https://datashare.is.ed.ac.uk/handle/10283/3571.

21. Gibson, L.; Rush, D. Novel Coronavirus in Cape Town Informal Settlements: Feasibility of Using Informal Dwelling Outlines to Identify High Risk Areas for COVID-19 Transmission From A Social Distancing Perspective. *JMIR Public Heal. Surveill* **2020**, *6*, e18844, doi:10.2196/18844.

22. Wang, Y.; Gibson, L.; Beshir, M.; Rush, D. Determination of critical separation distance between dwellings in informal settlements fire. *under Rev.*

23. Smith, H. M. The Relationship between Settlement Density and Informal Settlement Fires: Case Study of Imizamo Yethu, Hout Bay and Joe Slovo, Cape Town Metropolis BT - Geo-information for Disaster Management. In; van Oosterom, P., Zlatanova, S., Fendel, E. M., Eds.; Springer Berlin Heidelberg: Berlin, Heidelberg, 2005; pp. 1333–1355 ISBN 978-3-540-27468-1.

24. Asimakopoulou, E. K.; Kolaitis, D. I.; Founti, M. A. Thermal characteristics of externally venting flames and their effect on the exposed façade surface. *Fire Saf. J.* **2017**, *91*, 451–460, doi:10.1016/j.firesaf.2017.03.075.

25. Chen, A.; Francis, J. Radiant heat flux to external surfaces from escaping and extrusive flashover flames. *Proc. Inst. Mech. Eng. Part C J. Mech. Eng. Sci.* **2003**, *217*, 247–256, doi:10.1243/095440603762826567.

26. Cheng, H.; Hadjisophocleous, G. V. Experimental study and modeling of radiation from

compartment fires to adjacent buildings. *Fire Saf. J.* **2012**, *53*, 43–62, doi:10.1016/j.firesaf.2012.06.005.

27. Lee, S. W.; Davidson, R. A. Physics-based simulation model of post-earthquake fire spread. *J. Earthq. Eng.* **2010**, *14*, 670–687, doi:10.1080/13632460903336928.

28. Law, M.; O'Brien, T. *Fire Safety of Bare External Structural Steel*; Constrado: Croydon, 1981;

29. CEN *Eurocode 1: Actions on structures -Part 1: General actions - Actions on structures exposed to fire*; CEN, 2002; Vol. 2;.

30. Wang, Y.; Beshir, M.; Cicione, A.; Hadden, R.; Krajcovic, M.; Rush, D. A full-scale experimental study on single dwelling burning behavior of informal settlement. *Fire Saf. J.* **2020**, 103076, doi:10.1016/j.firesaf.2020.103076.

31. Huang, H.; Ooka, R.; Liu, N.; Zhang, L.; Deng, Z.; Kato, S. Experimental study of fire growth in a reduced-scale compartment under different approaching external wind conditions. *Fire Saf. J.* **2009**, *44*, 311–321, doi:10.1016/j.firesaf.2008.07.005.

32. Karlsson, B.; Quintiere, J. G. *Enclosure fire dynamics*; Gupta, A. K., Lilley, D. G., Eds.; CRC Press: London, New York, Washington D.C., 2000; ISBN 0849313007.

33. Glennie, D.; Hadjisophocleous, G. Calculation of radiant heat flux from compartment fires in various ventilation conditions. *MATEC Web Conf.* **2013**, *9*, doi:10.1051/matecconf/20130902006.

34. Wang, Y.; Bertrand, C.; Beshir, M.; Kahanji, C.; Walls, R.; Rush, D. Developing an experimental database of burning characteristics of combustible informal dwelling materials based on South African informal settlement investigation. *Fire Saf. J.* **2020**, *111*, 102938, doi:10.1016/j.firesaf.2019.102938.

35. Chen, H. X.; Liu, N. A.; Chow, W. K. Wind tunnel tests on compartment fires with crossflow ventilation. *J. Wind Eng. Ind. Aerodyn.* **2011**, *99*, 1025–1035, doi:10.1016/j.jweia.2011.07.006.

36. Chen, H.; Liu, N.; Zhang, L.; Deng, Z.; Huang, H. Experimental Study on Cross-ventilation Compartment Fire in the Wind Environment. *Fire Saf. Sci.* **2008**, *9*, 907–918, doi:10.3801/IAFSS.FSS.9-907.

37. de Koker, N.; Walls, R.; Cicione, A.; Sander, Z.; Loffel, S.; Claasen, J.; Fourie, S.; Croukamp, L.; Rush, D. 20 Dwelling Large-Scale Experiment of Fire Spread in Informal Settlements. *Fire Technol.* **2020**, doi:DOI 10.1007/s10694-019-00945-2.

38. Himoto, K.; Tanaka, T. Physics-based Modeling of Fire Spread in Densely-built Urban Area and its Application to Risk Assessment. *Monogr. la Real Acad. Ciencias Exactas, Físicas, Químicas y Nat. Zaragoza* **2010**, *34*, 87–104.

39. Tomar, S.; Kaur, A.; Sarma, K.; Dangi, H. K. Fire Risk Assessment and Fire Hazard Zonation Mapping using GIS in South-West Division of Delhi. *J. Adv. Res. Appl. Sci.* **2018**, *5*, 213–220.

40. Lao Urban Disaster Mitigation Project *Lao Urban Fire Risk Assessment Mapping in Vientiane Capital*; Viantiene, 2004;

41. Nisanci, R.; Yildirim, V.; Erbas, Y. S. Fire Analysis and Production of Fire Risk Maps : The Trabzon Experience. **2009**, *2005*.

42. Ferreira, T. M.; Vicente, R.; Raimundo Mendes da Silva, J. A.; Varum, H.; Costa, A.; Maio, R. Urban fire risk: Evaluation and emergency planning. *J. Cult. Herit.* **2016**, *20*, 739–745, doi:10.1016/j.culher.2016.01.011.

43. Zhao, S. Simulation of Mass Fire-Spread in Urban Densely Built Areas Based on Irregular

Coarse Cellular Automata. *Fire Technol.* **2011**, *47*, 721–749, doi:10.1007/s10694-010-0187-4.

44. Tan, E. E.; Vicente, A. J. Fire Spread Prediction Using Probabilistic Cellular Automata: the Case of Urban Settlements in the Philippines. *ISPRS - Int. Arch. Photogramm. Remote Sens. Spat. Inf. Sci.* **2019**, *42W1*, 415–420, doi:10.5194/isprs-archives-XLII-4-W19-415-2019.